

Development of magnetic materials and processing techniques applicable to integrated micromagnetic devices

J Y Park† and M G Allen

School of Electrical and Computer Engineering, Georgia Institute of Technology, Atlanta, GA 30332-0269, USA

Received 2 April 1998, accepted for publication 22 July 1998

Abstract. In this research, electroplated magnetically isotropic and anisotropic soft alloys and screen-printed soft ferrites applicable to micromachined micromagnetic devices are fabricated and characterized using *in situ* measurement techniques. Appropriate magnetic materials and deposition methods, such as electroplating and screen-printing techniques, are examined and material test structures are fabricated. Following material characterization, micromachined inductors with three-dimensional structure are fabricated to determine the usefulness of the magnetic materials and deposition methods. The micromachined inductor is a key component and geometry for realizing micromagnetic devices such as amplifiers, filters, sensors and actuators.

Three different material types are studied in this work. Electroplated magnetically isotropic soft alloys, permalloy (Ni80Fe20), orthonol (Ni50Fe50) and amorphous cobalt–iron–copper (CoFeCu) alloys, are studied, followed by electroplated magnetically anisotropic soft alloys of permalloy (Ni80Fe20) and supermalloy (NiFeMo), which have magnetically easy and hard axes. Finally, screen-printed polymers filled with soft ferrite (NiZn and MnZn) powders are fabricated and characterized.

1. Introduction

Many important signal and sensor/actuator applications require magnetic materials that have low hysteresis in the plot of the magnetic flux density of the material as a function of magnetic field intensity (B – H curve). Materials having this property are referred to as soft magnetic materials. A good soft magnetic material should have a large saturation magnetization to obtain a wide range of operation, and a high permeability to achieve a high magnetization even under a low applied field. It should also have a low coercivity and remanence, i.e., as mentioned above, a minimal hysteresis loop. Low magnetostriction and anisotropy are also recommended for stable magnetic anisotropy during deformation of the magnetic material. A low demagnetization is necessary for films of the material to easily become magnetically anisotropic at low applied magnetic field, allowing easy and hard axes to be clearly formed. Mechanical properties such as residual stress, hardness, tensile strength, friction coefficient, corrosion resistance, thermal conductivity, linear coefficient of expansion and adhesion properties may also be important for micromachined actuators.

For higher frequency applications, soft magnetic materials with high resistivity are appropriate to reduce eddy current losses [1]. Laminated alloy thin films can also reduce eddy current loss due to their increased resistivity. Although soft ferrites such as NiZn and MnZn ferrites are well known magnetic materials for conventional high frequency transformers and inductors, they are not compatible with many microfabrication processes, since their high sintering temperatures (1000 to 2000 °C [2]) are not compatible with many microfabrication steps.

In addition to appropriate material selection, it is also necessary to develop appropriate processing techniques for the incorporation of appropriate magnetic materials in micromachined magnetic devices. Many magnetic films are produced by methods such as vacuum evaporation [3], RF/magnetron sputtering [4, 5], rapid quenching from liquid metal, chemical vapor deposition [6], ion implantation, screen printing and spin casting [7] and electroplating [8, 9]. In this research, electroplating and composite screen-printing methods are chosen to obtain thick (above 5 μm) films with high deposition rate as well as due to the potential cost advantages of these processes, and due to their compatibility with many other micromachining fabrication sequences. Using electroplating techniques, magnetically isotropic and anisotropic supermalloy (NiFeMo), permalloy (Ni80Fe20), orthonol (Ni50Fe50), and amorphous alloys

† Phone: 404-894-8807. Fax: 404-894-5028.
E-mail: jae.park@ece.gatech.edu.

Table 1. Composition of electroplating solutions of permalloy (Ni80Fe20) and orthonol (Ni50Fe50).

Component	Ni (80%)–Fe (20%)	Ni (50%)–Fe (50%) ^a
NiSO ₄ ·6H ₂ O (g l ⁻¹)	200	168
FeSO ₄ ·7H ₂ O (g l ⁻¹)	8	81
NiCl ₂ ·6H ₂ O (g l ⁻¹)	5	135
H ₃ BO ₃ (g l ⁻¹)	25	50
Saccharin (g l ⁻¹)	3	3
pH	2.5–3.0	3.5–4.0
Temperature (°C)	25–30	55–60
Current density (mA cm ⁻²)	13	30

^a Optional stress-reduction additives were added (see text and table 3).

(CoFeCu) were deposited and characterized. Magnetically soft ferrite composites, consisting of NiZn and MnZn ferrites mixed with polymer binder, were deposited by screen-printing and spin-casting. The deposited composite materials were cured at low temperature and characterized prior to their incorporation in magnetic devices.

2. Magnetically soft, electroplated isotropic alloys

Among the many magnetic materials available in film form, NiFe and CoFe based alloys are attractive materials for realizing micromachined magnetic devices due to their favorable soft magnetic properties and their feasibility of deposition through electroplating. Permalloy (Ni80Fe20), orthonol (Ni50Fe50) and cobalt–iron–copper (CoFeCu) are investigated due to their good soft magnetic properties and a low magnetostriction. In particular, orthonol and CoFeCu alloys have very high saturation magnetization, 14–20 kG. In order to assess the suitability of these materials for micromachined devices, electrodeposited test samples are characterized using a vibrating sample magnetometer to test B – H characteristics, initial permeability, saturation flux density and coercivity.

2.1. Fabrication of test samples

Magnetic properties of bulk-type magnetic materials may be different from those of electrodeposited thin films. Thus, the magnetic properties measured from bulk-type magnetic samples can not always be used for designing micromachined magnetic devices. The magnetic properties of interest should be measured *in situ*, on as-deposited films. Test samples were prepared using surface micromachining techniques to meet the *in situ* measurement requirement.

As shown in figure 1, the fabrication procedure of the test samples is as follows. A seed layer consisting of 200 Å chromium, 4000 Å copper, and 400 Å chromium was deposited on a glass substrate using electron beam evaporation or sputtering to form both a sacrificial layer as well as an electroplating seed layer. A 20 μm thick photoresist layer (Shipley STR-1110) was spun on top of the seed layer and patterned to form electroplating sample molds. A mold of 20 μm thickness and 4 × 12 mm² area was achieved by two-step spin speeds: 1000 rpm for 15 seconds and then 3500 rpm for 5 seconds. After the photoresist was spun,

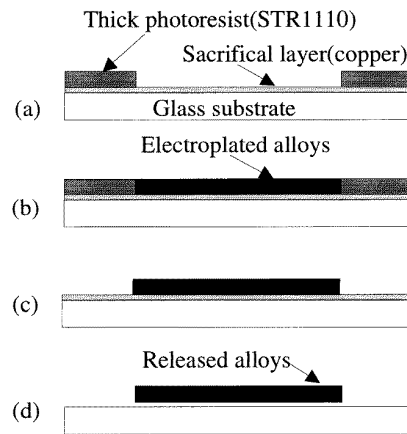


Figure 1. Fabrication sequence of the test samples for the *in situ* measurement of magnetic properties of magnetically isotropic soft alloys (permalloy, orthonol and CoFeCu alloys): (a) sacrificial layer and thick photoresist deposition; (b) electroplating of alloys; (c) removal of photoresist mold; (d) releasing of alloys.

Table 2. Electroplating solution and conditions of CoFeCu alloys.

Component	Quantity
CH ₃ COONa·3H ₂ O	11.05 (g l ⁻¹)
CoSO ₄ ·7H ₂ O	56.2 (g l ⁻¹)
FeSO ₄ ·7H ₂ O	5.5–8 (g l ⁻¹)
CuSO ₄ ·5H ₂ O	0.1–0.5 (g l ⁻¹)
H ₃ BO ₃	24.7 (g l ⁻¹)
Saccharin	3 (g l ⁻¹)
pH	2.5–4
Temperature	25–30 (°C)
Current density	7 (mA cm ⁻²)

the substrate was left at room temperature for above 3 minutes. The photoresist was then soft baked in two steps: a 70 °C hot plate for 4 minutes followed by 105 °C for 4 minutes. The resist was exposed and developed to form electroplating molds. After removing the top seed layer, the electroplating molds were filled with the magnetic alloys to be tested, using electroplating techniques and the parameters in tables 1 and 2.

To prepare the nickel–iron electroplating bath, a glass

Table 3. Addition agents for orthonol plating solutions.

M&T nickel-iron stabilizer	4.5 g l ⁻¹
M&T nickel-iron additive NI-2	20 ml l ⁻¹
M&T nickel-iron additive NI-3	40 ml l ⁻¹
M&T wetting agent Y-17 (air)	1.5 ml l ⁻¹
M&T wetting agent Y-11 (mechanical)	1.5 ml l ⁻¹

beaker of 1000 ml was cleaned by using TCE, acetone, methanol and de-ionized (DI) water in sequence. The alloy plating chemicals described in table 1 and table 2 were weighed and then mixed in the glass beaker. DI water was added to fill the glass beaker to 1000 ml, and the electroplating solution was stirred slowly for a day with a Teflon propeller blade to ensure dissolution.

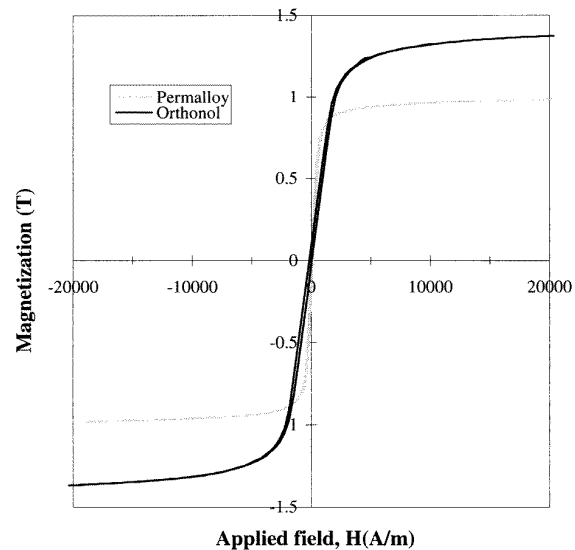
Pure nickel metal film was used as an anode electrode for plating permalloy and orthonol magnetic films, while a pure cobalt metal film was used for CoFeCu alloys. By using non-magnetic copper clips, electrical contact was made to the nickel or cobalt anode as well as the seed layer, and the nickel or cobalt anode and the plating substrate were then immersed in the well mixed plating solution to plate the magnetic alloys. A DC power supply (HP 6622A) which had both voltage and current adjustments was used as a power source for the electroplating. The anode and the substrate were connected to the positive and negative terminal of the dc power supply respectively. During the electroplating operation, the solution was maintained at appropriate temperature and pH, together with the other conditions described in tables 1 and 2. To plate the orthonol material, various additives from M&T Chemicals, Inc. were used to control internal stress and ductility of the deposit, to keep the iron content solublized and to obtain bright films and leveling of the process as described in table 3. Air agitation and saccharin were also added to reduce internal stress and to keep the iron content stabilized.

Upon completion of electroplating, the sacrificial seed layer was selectively wet etched to release the test samples from the substrate.

2.2. *In situ* measurement of isotropic alloy properties and applications

The compositions of the electroplated alloys were measured by energy dispersion spectroscopy (EDS). Table 4 shows that the compositions of the plated magnetic alloy films were very close to the expected composition. Figure 2 shows the magnetic $B-H$ (magnetic flux density-applied field strength) characteristics of electroplated permalloy and orthonol magnetic films. Both materials exhibit a relatively high permeability. The saturation flux density (B_s) for the electroplated permalloy samples was approximately 0.9 T, while the saturation flux density for the orthonol samples was approximately 1.4 T. As shown in figure 2, the slope of the magnetization curve in its linear region is larger for the permalloy than for the orthonol.

The compositions of the plated CoFeCu alloys shown in table 5 were obtained by varying the amount of cupric sulfate ($\text{CuSO}_4 \cdot 5\text{H}_2\text{O}$) and iron sulfate ($\text{FeSO}_4 \cdot 7\text{H}_2\text{O}$) in

**Figure 2.** Magnetization versus magnetic field intensity curve for fabricated permalloy and orthonol test samples.

the plating solution as shown in table 2. As copper concentration in the plated film decreased, both cobalt and iron concentration, as well as the saturation magnetization, increased. As shown in table 5, CoFe alloys had higher saturation flux density than CoFeCu alloys, while CoFeCu alloys had lower coercivity than CoFe alloys. CoFeCu alloy with 9.8% copper composition had the lowest coercivity. Figure 3 shows $M-H$ characteristics (magnetization versus applied field) of test samples 2, 3 and 4 to compare magnetic characteristics of electroplated CoFe alloys and CoFeCu alloys. Regarding the electroplated CoFeCu alloys, the measured slope of the magnetization curve in its linear region of the sample 2 was the highest, of sample 3 was the lowest, and of sample 4 was intermediate. Plated CoFeCu alloys had higher initial relative permeability than CoFe alloys. In the electroplated magnetic alloys, supermalloy, orthonol and CoFeCu, the content of Fe affected the saturation magnetization. The amount of Fe can be increased to obtain high saturation magnetization, at the expense of increasing coercivity.

Micromachined inductors with plated permalloy and orthonol cores were fabricated to demonstrate the usefulness of both the materials and the deposition methods for realizing micromagnetic devices [10]. Figures 4 and 5 show scanning electron micrograph (SEM) pictures of fabricated bar-type micromachined inductors. Figure 6 shows the inductance and quality factor of micromachined inductors with plated permalloy and orthonol cores. For an inductor size of 4 mm \times 1.0 mm in area and 0.13 mm thickness having 30 turns of multilevel coils, the achieved inductances were approximately 0.67 μH for the inductor with permalloy core and 0.57 μH for the inductor with orthonol core at low frequencies (100 kHz). As seen, the permalloy core inductor has a slightly higher inductance and Q -factor than the orthonol core inductor, which corresponds to the measured magnetic properties of plated permalloy and orthonol films.

Table 4. Compositions and magnetic properties of electroplated permalloy and orthonol alloys.

Samples	Measured composition (wt%)	Under layer	Saturation magnetization (T)	Coercivity (Oe)
Permalloy	Ni79.8Fe20.2	Cu	0.9	0.65
Orthonol	Ni50.9Fe49.1	Cu	1.41	1.3

Table 5. Compositions and magnetic properties of electroplated CoFeCu alloys.

Samples	Measured composition (wt%)	Under layer	Saturation magnetization (kG)	Coercivity (Oe)
1	Co80.5Fe1.8Cu17.7	Cu	13.0	6.1
2	Co83.2Fe7.0Cu9.8	Cu	14.6	2.8
3	Co86.7Fe8.3Cu5	Cu	15.5	4.9
4	Co89.3Fe10.7	Cu	16.4	10.7

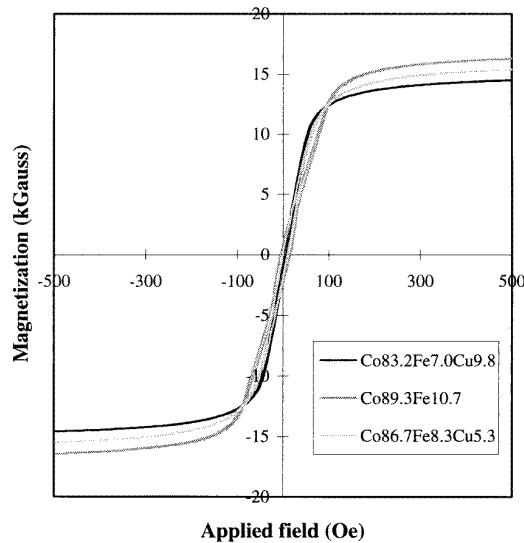


Figure 3. Magnetization as a function of applied magnetic field of fabricated CoFeCu alloy films.

3. Electroplated soft alloys with magnetically anisotropic properties

In certain ranges of high frequencies, some magnetic materials suffer from a decrease in effective permeability [11–13]. In these cases, anisotropic magnetic materials (i.e., materials with a magnetically hard and easy axis in the plane of the film, formed, e.g., by application of a directional magnetic field during electrodeposition) are often employed, since the magnetic properties of the film are often more stable in the hard axis direction at higher frequencies [14–17]. For example, the easy axis (the in-plane direction of the plated film parallel to the applied magnetic field during plating) of an anisotropic magnetic film has a high permeability at low frequency and is therefore often used for low frequency applications, while the hard axis (the in-plane direction of the film perpendicular to the applied magnetic field)

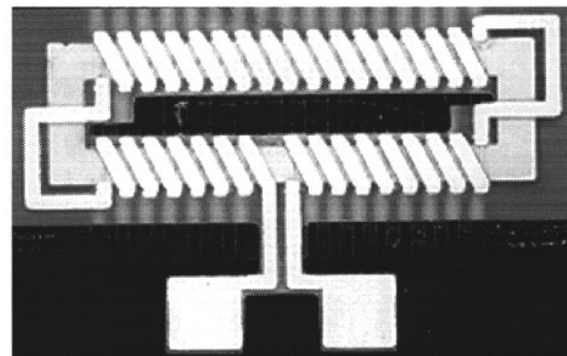


Figure 4. Photomicrograph of a fabricated micromachined inductor. The dimension of the integrated inductor is 4 mm in length, 1 mm in width and 0.13 mm in height.

is often used for high frequency applications. In order to improve the high frequency characteristics of the ‘bar type’ inductor discussed above [10,18], new processing techniques to combine the processes for the fabrication of these devices with magnetically anisotropic materials are required. To demonstrate this approach, permalloy [19–21] and supermalloy [22–24] were electroplated in a magnetic field and evaluated as magnetic core materials in test devices. To reduce the demagnetizing field during the electroplating, appropriate electroplating mold patterns [25] and etching techniques for the plated magnetic films were used.

3.1. Fabrication of test samples

Figure 7 shows the fabrication sequence of test samples of both permalloy and supermalloy with magnetically anisotropic properties. A seed layer consisting of 200 Å chromium, 5000 Å copper and 400 Å chromium was deposited on a glass substrate using electron beam evaporation to form a sacrificial layer and an electroplating seed layer. A 5 μm thick photoresist layer (Shipley STR-1110) was spun on top of the seed layer and patterned

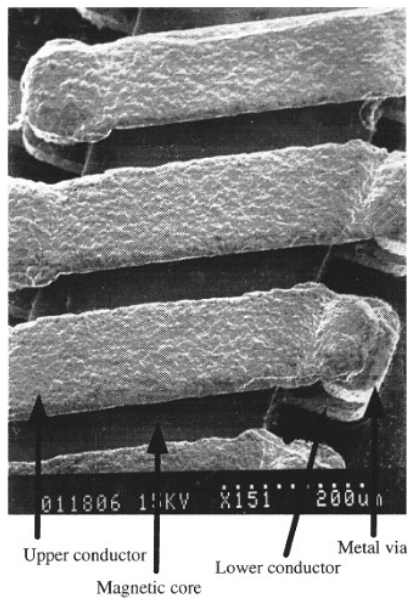


Figure 5. Scanning electron micrograph of the wrapped conductors and the core of the micromachined inductor.

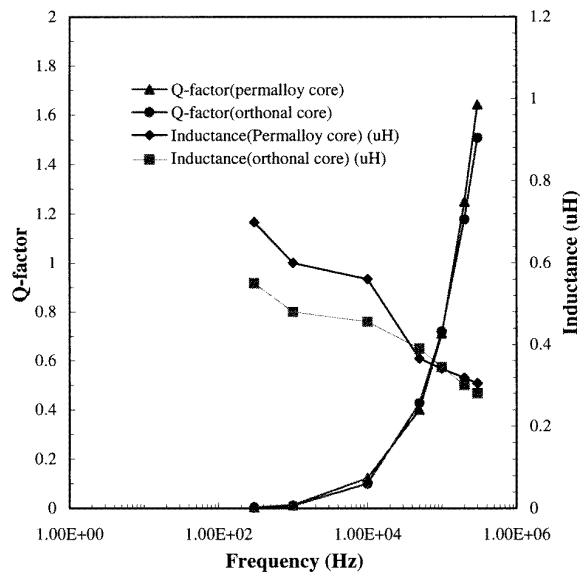


Figure 6. Comparison of inductance and quality factor of a micromachined inductor with plated magnetically isotropic permalloy and orthonol cores.

to form electroplating molds with narrow walls ($15 \mu\text{m}$). The $5 \mu\text{m}$ thick mold was achieved by a two-step spin speed: 2000 rpm for 15 seconds followed by 4000 rpm for 10 seconds. After the photoresist was spun, the substrate was left at room temperature for above 3 minutes. The photoresist was then soft baked in two steps: 70°C on a hot plate for 3 minutes followed by 105°C for 3 minutes. The photoresist was exposed and developed to form plating molds for the samples, as well as plated flux guides for the introduction of magnetic anisotropy. After removing the top seed layer, the electroplating molds were filled with electroplated permalloy and supermalloy magnetic

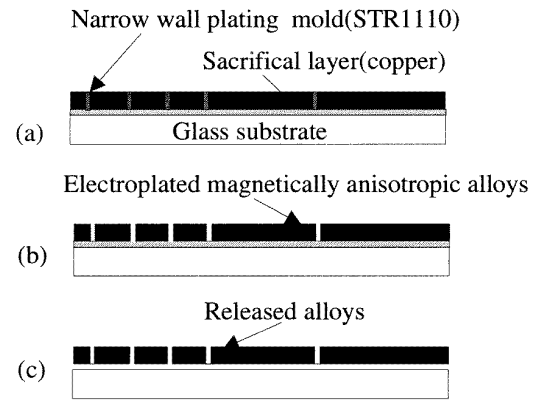


Figure 7. Fabrication sequence of the test samples for the *in situ* measurement of magnetic properties of magnetically anisotropic soft alloys (permalloy and supermalloy): (a) deposition of sacrificial layer and thick photoresist with narrow wall on a glass substrate; (b) electroplating of alloys under applied magnetic field; (c) removal of photoresist and releasing of alloys using wet etching.

Table 6. Electroplating solution and conditions of supermalloy alloys.

Chemicals and conditions	Quantity
$\text{NiSO}_4 \cdot 6\text{H}_2\text{O}$	$60 \text{ (g l}^{-1}\text{)}$
$\text{FeSO}_4 \cdot 7\text{H}_2\text{O}$	$4 \text{ (g l}^{-1}\text{)}$
$\text{Na}_2\text{MoO}_4 \cdot 2\text{H}_2\text{O}$	$2 \text{ (g l}^{-1}\text{)}$
NaCl	$10 \text{ (g l}^{-1}\text{)}$
Saccharin	$3 \text{ (g l}^{-1}\text{)}$
Citric acid	$66 \text{ (g l}^{-1}\text{)}$
Temperature	$25\text{--}30 \text{ (}^\circ\text{C)}$
Current density	$10\text{--}15 \text{ (mA cm}^{-2}\text{)}$

alloys. To obtain anisotropic magnetic characteristics, a magnetic field was applied in the in-plane direction of the film during plating. A magnetic field strong enough to overcome the demagnetizing field of the films being plated should be applied during deposition to achieve magnetically anisotropic films. Thus, NdFeB magnets ($BH_{\text{max}} = 35 \text{ MG Oe}$), along with a carefully designed iron yoke, were employed. Permalloy ($\text{Ni}_{80}\text{Fe}_{20}$) films were plated under the influence of a 300 mT applied magnetic field, while supermalloy (NiFeMo) films were plated under the influence of a 50 mT applied magnetic field. The compositions and conditions of electroplating are described in tables 1 and 6. A nickel foil was used as an anode during the electroplating of both permalloy and supermalloy films. As shown in tables 1 and 6, no heating was employed during the electroplating processes, and stirring was performed. After electroplating, the photoresist mold was removed using acetone and the seed layer was selectively wet etched, releasing the plated alloy samples from the substrate.

3.2. *In situ* measurement of anisotropic alloy properties and applications

The magnetic properties of the anisotropic films were measured using a vibrating sample magnetometer as well

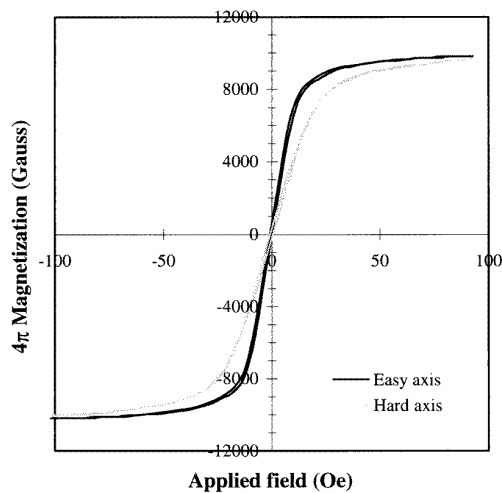


Figure 8. Magnetization as a function of applied magnetic field of electroplated magnetically anisotropic permalloy film.

as a permeameter. Figure 8 shows the magnetic $M-H$ characteristics of electroplated permalloy (Ni80Fe20) magnetic films with easy and hard axes. The plated magnetically anisotropic permalloy films exhibit a higher permeability than their isotropic counterparts discussed previously. Regarding the magnetically anisotropic permalloy samples shown in figure 8, the measured slope of the magnetization curve in its linear region for the easy axis direction was higher than for the hard axis direction at low frequency. The coercivity of the plated samples was 0.402 Oe and 0.635 Oe along the easy and hard axes respectively. The saturation magnetization, M_s for these electroplated permalloy samples ranged from 0.9 to 1.0 T. Figure 9 shows the magnetic $M-H$ (magnetization versus applied field strength) characteristics of electroplated supermalloy (NiFeMo) magnetic films with easy and hard axes. The plated magnetically anisotropic supermalloy films also have a relatively high permeability. Regarding the magnetically anisotropic supermalloy samples shown in figure 9, the measured slope of the magnetization curve in its linear region for the easy axis direction was higher than for the hard axis direction at low frequency. The coercivity of the easy and hard axes of the plated samples was 0.556 Oe and 0.715 Oe respectively. The saturation magnetization, M_s for the electroplated anisotropic supermalloy samples was 0.8 T. The plated films showed increased nickel and molybdenum concentrations over what was expected, and a decrease of the coercivity when the film is plated in the presence of an applied magnetic field. Supermalloy (NiFeMo) has higher permeability than permalloy (NiFe), while permalloy has higher saturation magnetization than supermalloy. In our experiments, supermalloy could not be plated thicker than 5 μm without cracking and adhesion loss, while permalloy could be plated much thicker than 50 μm .

The permeability of the easy axis was much higher than that of the hard axis at low frequency. However, the measured permeability of the easy axis fell as frequency was increased, while the permeability of the hard axis

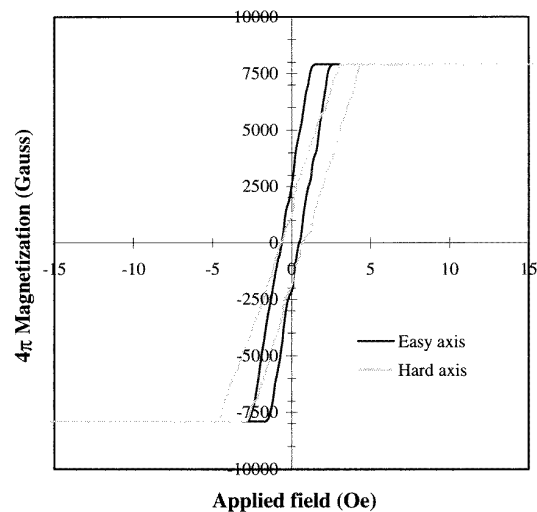


Figure 9. Magnetization as a function of applied magnetic field for an electroplated magnetically anisotropic supermalloy film. Note the very small values of the horizontal scale.

remained constant up to 1 MHz and higher [24]. Thus, the magnetic characteristics of the hard axis were investigated for integrated micromagnetic devices operating at high frequencies.

Micromachined inductors with plated magnetically anisotropic supermalloy cores were fabricated to verify the suitability of these materials in micromagnetic devices. Figures 10 and 11 show photomicrographs of batch fabricated micromachined inductors with magnetically anisotropic cores. Easy axis core and hard axis core devices were fabricated simultaneously [26]. Figure 12 shows the inductance and quality factor of micromachined inductors with plated magnetically anisotropic supermalloy cores. The inductors have an inductor size of 2.4 mm \times 1.4 mm, cross-sectional core area of 0.5 mm \times 0.004 mm and 32 turns of multilevel coils 40 μm in width, 15 μm in thickness and 20 μm in spacing. Figure 12 shows that micromachined inductors with magnetically anisotropic cores have high inductance due to their increased permeability even though they have a relatively thin magnetic core. As shown in figure 12, the inductor with easy axis core has good performance at low frequencies, while the hard axis core inductor has better performance at high frequencies. The favorable magnetic properties of plated magnetically anisotropic films may be useful not only for micromachined inductors, but also for other microsensors and microactuators.

4. Screen-printed soft ferrite composite (polymer-filled ferrite)

Although bulk ferrite materials have suitable soft magnetic properties for high frequency applications, their deposition usually require high temperatures, pressing and sintering. Magnetic polymer composites, in which small particles of magnetic materials are suspended in a nonmagnetic (e.g., polymeric) matrix or binder, offer a good compromise

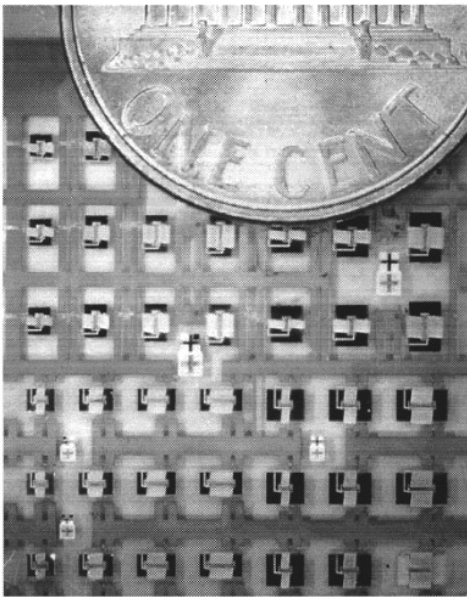


Figure 10. Photomicrograph of the batch fabricated micromachined inductors with magnetically anisotropic cores.

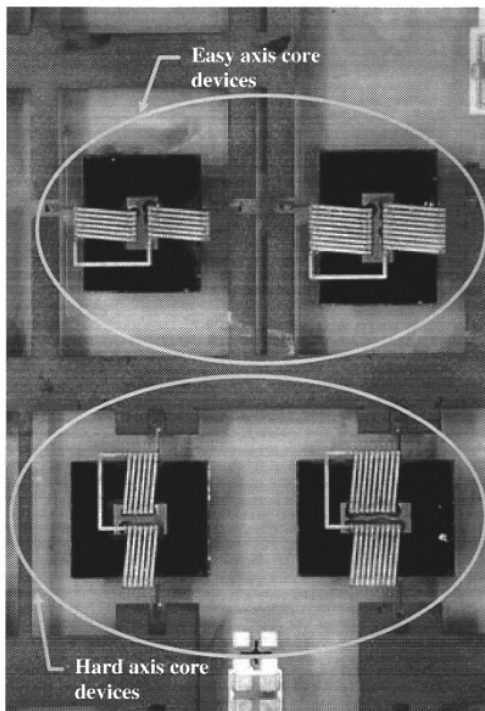


Figure 11. Photomicrograph of the integrated micromachined inductors with magnetically anisotropic cores of easy and hard axes including signal and ground pads: easy axis devices at top and hard axis devices at bottom.

to combine the favorable properties of the magnetic materials with the simple processing sequences of the polymer. Three types of polymer binder can be used: elastomeric, thermoplastic and thermoset. The choice of the polymer matrix depends on its ability to accept

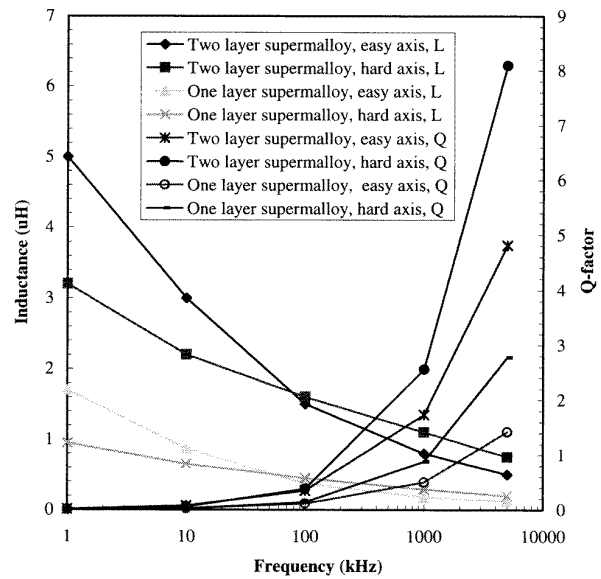


Figure 12. Comparison of inductance and quality factor of micromachined inductors with plated magnetically anisotropic supermalloy cores.

large volume loading of magnetic powder; its thermal, chemical and mechanical properties and the type of process used to apply the composite. Polyimides are useful in microelectronics applications due to their good insulating properties, good adhesion properties and low relative permittivity. Polyimides are widely used in the fabrication of micromachined devices and integrated circuits as insulating and planarization materials. Polyimides can be also mixed with conductive, resistive, dielectric, and magnetic powders to form polymer–matrix composites. Magnetic composite materials in which powder alloys, ferrites and other magnetic powders are mixed with polymer binders are applicable to micromachined magnetic devices due to the ease of deposition of such composites by spin-casting or screen-printing. The composite materials have various advantages such as higher volume production and possible production of complicated small and thick shapes. Thus, their applications are wide ranging. The magnetic properties of the composite are strongly dependent on the intrinsic magnetic properties of the incorporated magnetic powder, the concentration of the magnetic powder and its degree of orientation in the polymer matrix. The degree of orientation is affected by the interaction between polymer matrix and magnetic powder, and the viscoelastic properties of the matrix.

Magnetically soft NiZn and MnZn ferrites are widely used as core materials for high frequency inductors and transformers in miniaturized power supply applications. Since they have higher resistivity than other magnetic materials, eddy current losses that can be large at high frequencies in metal-core inductors are reduced. The NiZn ferrites studied here have lower permeability and higher bulk or volume resistivity than their MnZn counterparts.

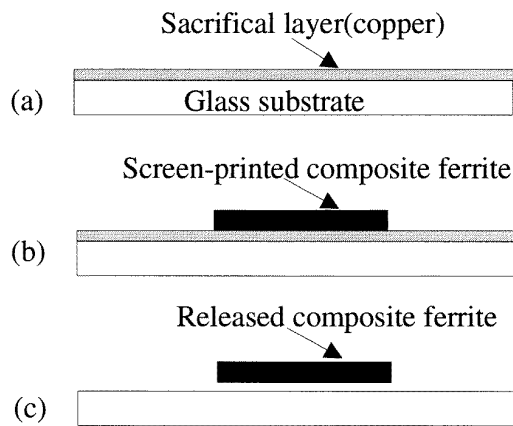


Figure 13. Fabrication sequence of the test samples for the *in situ* measurement of magnetic properties of screen-printed ferrite composites (NiZn and MnZn): (a) deposition of sacrificial layer on a glass substrate using an electroplating technique; (b) screen printing of ferrite composite through a patterned mask; (c) releasing of testing sample using wet etching.

4.1. Fabrication of test samples

In this work, the polyimide PI-2555 from Dupont (a benzophenone tetracarboxylic dianhydric-oxydianiline/metaphenylene formulation) was used as the binder material. Although the recommended curing temperature of this polyimide (300–350 °C) is high, longer cure times at lower temperatures, or use of a preimidized material, can lower the required processing temperatures. Other microelectronics-compatible materials, such as epoxies and polynorbornenes, are also suitable candidates as binder materials. The ceramic ferrites employed were 1.2 μm NiZn and 0.8 μm MnZn ferrite particles produced by the Steward Company. Suitable dispersion agents were employed to enhance uniformity of the composite suspension.

The composite material was prepared by mixing measured quantities of PI-2555 polymer binder, ferrite particles, dispersion agents and a few ceramic balls in a container and placing the container in a ball mill rotator for at least 48 hours to ensure homogeneity of the mixed composite solution. The well mixed composite material was deposited by either screen-printing or by spin-casting followed by photolithography. Due to the difficulty of etching the thick composite films to form patterns after being deposited by spin-casting, the screen-printing method is preferred. The deposited films are cured at 160–300 °C to achieve final properties.

Figure 13 shows the fabrication sequences of a test sample of ferrite composite material. The process started with a glass substrate, onto which 200 Å chromium, 2000 Å copper and 400 Å chromium were deposited. Onto this substrate, a 10 μm thick copper layer was deposited using electroplating to form a sacrificial layer. The thick sacrificial layer was needed due to the relatively thick and wide test samples of the screen-printed ferrite composite. The composite was then screen-printed on the electroplated sacrificial layer through a square 4 mm \times 4 mm opening in the screen. The screen-printed composite material was soft

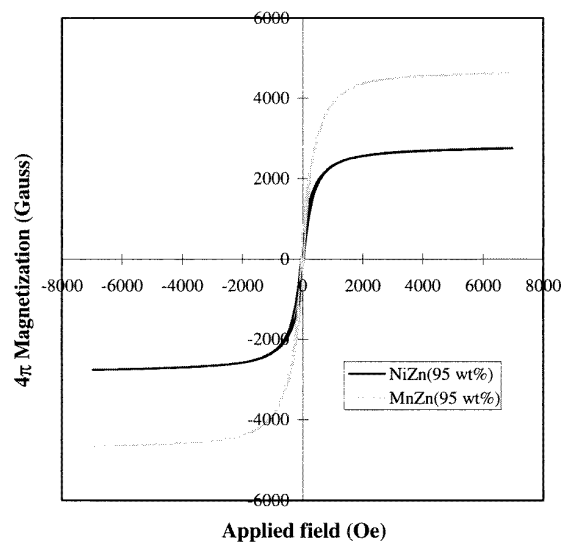


Figure 14. Comparison of magnetization and applied magnetic field of screen-printed ferrite composites.

baked for 10 minutes at 120 °C and hard cured at 300 °C for 1 hour in nitrogen, yielding an after-cure thickness of 50 μm . The thickness of the screen-printed composite materials is dependent on the thickness of the emulsion of the screen used during the deposition. After curing the ferrite composite, the copper sacrificial layer was wet etched and test samples were released from the substrate.

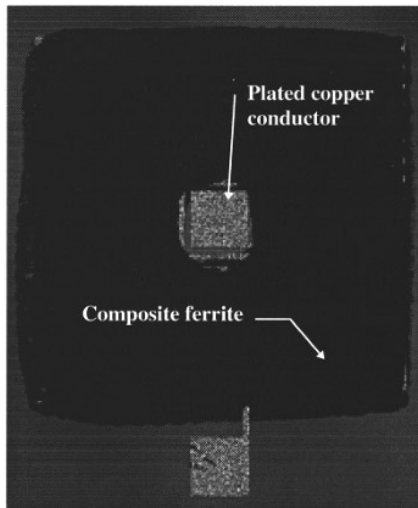
4.2. Measurement of ferrite composite magnetic properties and applications

In addition to the requisite magnetic properties, the significant electrical properties of the ferrite-based magnetic materials to be measured are electrical resistivity and dielectric constant. The electrical properties of the fabricated test samples (95 wt% ferrite) were measured using a Philips PM 2525 multimeter and a Keithley 3322 LCZ meter. The electrical resistivity of the NiZn ferrite composite was approximately 1 M Ω cm and that of the MnZn ferrite composite was approximately 0.01 M Ω cm. The magnetic properties of screen-printed composite materials were characterized using a vibrating sample magnetometer. The measured sample shows the MnZn ferrite composite material has higher saturation flux density ($B_s = 0.43$ T) and relative permeability than the NiZn ferrite composite material ($B_s = 0.28$ T) as shown in figure 14. The fabricated magnetic composite ferrite material has inferior magnetic properties compared to bulk sintered ferrite as shown in table 7, perhaps due to the presence of the polyimide binder and the degree of orientation of the magnetic powder in the composite compared with that of bulk sintered ferrite [27].

Figure 15 shows photomicrographs of an EMI shielded micromachined inductor with ferrite composite magnetic material and spiral type coils with dimensions: 2.6 mm \times 2.6 mm \times 70 μm [28]. As shown in figure 16, the integrated inductors incorporating MnZn ferrite composite have higher inductance than the corresponding NiZn ferrite composite

Table 7. Comparison of bulk and composite ferrite magnetic materials.

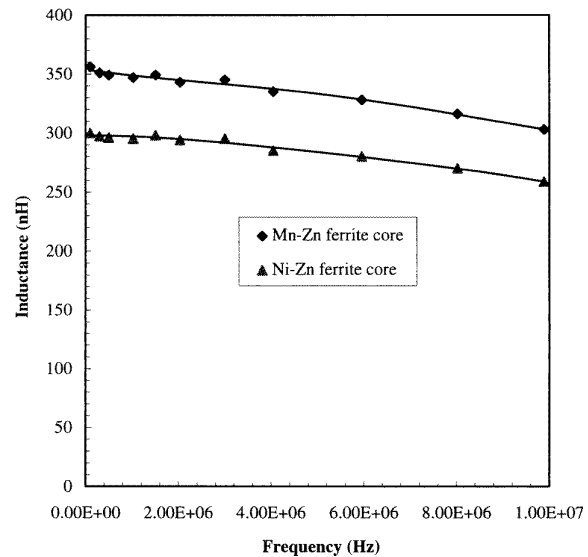
Parameter type	NiZn ferrite		MnZn ferrite	
	Composite	Bulk	Composite	Bulk
B_s (Gauss)	2900	3250	4300	4700
Resistivity (Ω cm)	10^6	10^5	10^4	5×10^2

**Figure 15.** Photomicrograph of an EMI shielded micromachined inductor with screen-printed ferrite composite and plated spiral type coils: dimensions: $2.6 \text{ mm} \times 2.6 \text{ mm} \times 70 \mu\text{m}$.

devices, corresponding to the $B-H$ characteristics of fabricated composite core materials. The integrated spiral inductors without magnetic composite materials have approximately 230 nH of inductance.

5. Conclusions

In this research, appropriate magnetic materials were selected for micromachined magnetic device applications based on achievable magnetic properties as well as compatibility of their deposition processes with micromachining techniques. Magnetically isotropic metal NiFe and NiFeCo alloys, magnetically anisotropic NiFe and NiFeMo alloys and ferrite/polymer composites were investigated. Electrodeposition and screen printing were selected as particularly appropriate micromachining-compatible deposition means for these materials. To demonstrate the efficacy of these materials and deposition processes, inductor structures incorporating these materials in the inductor core were designed, fabricated and tested. Based on the materials characterization results and the electrical performance of the inductor test structures, it is concluded that the magnetic materials described in this paper have high feasibility and potential for integrated magnetic device applications.

**Figure 16.** Comparison of inductance of EMI shielded sandwich type spiral inductors with dimension $2.6 \text{ mm} \times 2.6 \text{ mm} \times 70 \mu\text{m}$ and 12 turns.

Acknowledgments

This research was supported by the National Science Foundation through the Georgia Tech/NSF Engineering Research Center in Electronic Packaging (contract EEC-9402723). Materials donations by E I DuPont de Nemours & Co. and M&T Chemicals Inc. are also gratefully acknowledged. Microfabrication was carried out at the Microelectronics Research Center of Georgia Tech with the assistance of the staff. Assistance with measurement of magnetic properties of materials from Dr William Taylor of Georgia Tech as well as Dr Michael Schneider and Professor Henry Baltes of the Swiss Federal Institute of Technology (ETH-Zürich) is gratefully acknowledged. Valuable technical discussions and assistance in fabrication and measurement of CoFeCu alloys and magnetically anisotropic films from Dr S H Han of the Korea Institute of Technology in Korea are also greatly appreciated.

References

- [1] Littmann M 1971 Iron and silicon-iron alloys *IEEE Trans. Magn.* **7** 48–57
- [2] Snelling E 1988 *Soft Ferrites, Properties, and Applications* 2nd edn (London: Butterworths)
- [3] Hasiwa T and Matsumoto M 1988 Fe-Co-P thin films prepared with a reactive evaporation method *IEEE Trans. Magn.* **24** 2055–8
- [4] Sakurai T, Kitakami O and Shimada Y 1994 Observation of high density recording states using magnetic fine particles made by sputtering method *J. Magn. Magn. Mater.* **130** 384–90
- [5] Hanazono M, Narishige S and Kawakami K 1982 Fabrication of a thin film head using polyimide resin and sputtered Ni-Fe films *J. Appl. Phys.* **64** 2608–10
- [6] Lane P, Cockayne B, Wright P and Oliver P 1994 Metalorganic chemical vapor deposition of manganese arsenide for thin film magnetic applications *J. Cryst. Growth* **143** 237–42

- [7] Lagorce L and Allen M 1997 Magnetic and mechanical properties of micromachined strontium ferrite/polyimide composites *IEEE J. Microelectromech. Syst.* **6** 307–12
- [8] Hironaka K and Uedaira S 1990 Soft magnetic properties of Co–Fe–P and Co–Fe–Sn–P amorphous films formed by electroplating *IEEE Trans. Magn.* **26** 2421–3
- [9] Raman V, Williams E and Schenoi B 1982 Some property data for nickel–iron alloy electrodeposits *Plating Surf. Finishing* 132–6
- [10] Park J and Allen M 1996 A comparison of micromachined inductors with different magnetic core materials *IEEE 46th ECTC Conf.* pp 375–81
- [11] Grossner N 1983 *Transformers for Electronic Circuits* 2nd edn (New York: McGraw-Hill)
- [12] Masi J and Thibault W 1995 New, high frequency transformer topologies *Proc. Electrical/Electronic Insulation Conf.* pp 157–61
- [13] Riahi-kashani M and Elshabini-Raid A 1992 Permeability evaluation of ferrite pastes, epoxies and substrates over a wide range of frequencies *IEEE Trans. Instrum. Meas.* **41** 1036–40
- [14] Vermeulen J, Acher O and Ravel F 1993 Microwave permeability and structural properties of CoFeSiB alloys prepared by ion beam sputtering *J. Appl. Phys.* **73** 6620
- [15] Han S, Kim K, Kim H and Kang I 1990 Magnetic properties of amorphous Co–Y thin film alloys *J. Korean Inst. Met.* **28** 957–63
- [16] Grimes C and Lumpp J 1996 The soft magnetic properties of stripes fabricated using laser ablation of multilayer thin films *J. Appl. Phys.* **79** 5497–9
- [17] Jin S, Zhu W, Tiefel T and Korenivski V 1997 High frequency properties of Fe–Cr–Ta–N soft magnetic films *J. Appl. Phys. Lett.* **70** 3161–3
- [18] Ahn C, Kim Y and Allen M 1996 A comparison of two micromachined inductors (bar and meander type) for fully integrated boost DC/DC power converters *IEEE Trans. Power Electron.* 239–45
- [19] Taylor W P, Brand O and Allen M G 1998 Fully integrated magnetically actuated micromachined relays *IEEE J. Microelectromech. Syst.* **7** 181–91
- [20] Schneider M, Castagnetti R, Allen M G and Baltes H 1995 Integrated flux concentrator improves CMOS magnetotransistor *Proc. IEEE Micro Electro Mechanical Systems Workshop (Amsterdam)* pp 151–6
- [21] Choi S, Kawahito S, Matsumo Y, Ishida M and Tadokoro T 1996 An integrated micro flux fluxgate magnetic sensor *Sensors Actuators A* **55** 121–6
- [22] Freitag W and Mathias J 1965 Electrodeposited nickel–iron–molybdenum thin magnetic films *J. Electrochem. Soc.* **112** 64–7
- [23] Shinoura O 1995 Electrodeposition of Ni–Fe–Mo multilayered soft magnetic films with high specific resistance *Denki Kagaku* **63** 473–8
- [24] Taylor W, Schneider M, Baltes H and Allen M 1997 Electroplated soft magnetic materials for microsensors and microactuators *Proc. Transducers'97 (Chicago, IL)* pp 1445–8
- [25] Romankiw L, Croll I and Hatzakis M 1970 Batch fabricated thin film magnetic recording heads *IEEE Trans. Magn.* **6** 597–9
- [26] Park J, Han S, Taylor W and Allen M 1998 Fully integrated micromachined inductors with electroplated anisotropic magnetic cores *IEEE 13th Applied Power Electronics Conf. (CA)*
- [27] Kawauchi K 1988 Effect of polymer matrices on magnetic properties *J. Mater. Sci.* **23** 2637–44
- [28] Park J Y, Lagorce L K and Allen M G 1997 Ferrite-based integrated planar inductors and transformers fabricated at low temperature *IEEE Trans. Magn.* **33** 3322–5